ARCTIC
VOL. 65, SUPPL. 1 (2012) P. 43–58

Morphology and Development of Ice Patches in Northwest Territories, Canada

THOMAS MEULENDYK,[1,2] BRIAN J. MOORMAN,[1] THOMAS D. ANDREWS[3] and GLEN MacKAY[3]

(*Received 22 February 2011; accepted in revised form 28 November 2011*)

ABSTRACT. Permanent ice patches in the western Canadian Subarctic have been recently identified as sources of cryogenically preserved artifacts and biological specimens. The formation, composition, and constancy of these ice patches have yet to be studied. As part of the Northwest Territories (NWT) Ice Patch Study, ground-penetrating radar (GPR) and ice coring were used to examine the stratigraphy and internal structure of two ice patches. Results show the patches are composed of a core of distinct offset units, up to several metres thick, covered by a blanket of firn and snow. The interfaces between the units of ice are often demarcated by thin sections of frozen caribou dung and fine sediment. Radiocarbon dates of dung extracted from ice cores have revealed a long history for these perennial patches, up to 4400 years BP. Ice patch growth is discontinuous and occurs intermittently. Extensive time gaps exist between the units of ice, indicating that summers of catastrophic melt can interrupt extended periods of net accumulation. The results of this work not only display the character of ice patch development, but also indicate the significant role that ice patches can play in reconstructing the paleoenvironmental conditions of an area.

Key words: Holocene, ground-penetrating radar, ice coring, radiocarbon dating, geomorphology, ice accumulation, dung, firn

RÉSUMÉ. Récemment, on a déterminé que les névés permanents du subarctique de l'Ouest canadien constituent des sources d'artefacts et de spécimens biologiques préservés cryogéniquement. La formation, la composition et la constance de ces névés n'ont toujours pas été étudiées. Dans le cadre de l'étude des névés des Territoires du Nord-Ouest, on a recouru à des géoradars (GPR) et au carottage de la glace pour examiner la stratigraphie et la structure interne de deux névés. Les résultats indiquent que les névés sont composés d'un noyau d'unités distinctes et décalées, mesurant plusieurs mètres d'épaisseur et recouvertes d'une couverture de vieille neige et de neige. L'interface entre les unités de glace est souvent démarquée par de minces sections de déjections de caribou gelées et de sédiments fins. La datation au radiocarbone des déjections extraites des carottes de glace révèle que ces névés pérennes ont une longue histoire, remontant jusqu'à 4400 ans BP. L'amplification des névés est discontinue et se produit de manière intermittente. Des écarts de temps considérables existent entre les unités de glace, ce qui laisse entendre que des étés de fonte catastrophique peuvent interrompre les périodes prolongées d'accumulation nette. Les résultats de cette étude laissent non seulement entrevoir le caractère de la formation des névés, mais indiquent également le rôle important que les névés peuvent jouer dans la reconstruction des conditions paléoenvironnementales d'une région.

Mots clés : Holocène, géoradar, carottage de la glace, datation au radiocarbone, géomorphologie, accumulation de glace, déjection, névé

Traduit pour la revue *Arctic* par Nicole Giguère.

INTRODUCTION

Ice patches are areas of permanent ice, often with a layer of snow cover, found in alpine regions on slopes that face northwest, north, or northeast (Washburn, 1979). Usually formed in depressions, ice patches vary from 100 m to 1 km in length and from 10 to 80 m in height. Ice patches differ from glaciers in that they do not acquire enough mass to flow (Glen, 1955). They form as annual accumulations of snow are gradually compressed into permanent ice lenses. The process of ice patch formation is still poorly understood, but it may be revealed through a study of internal ice patch structure.

Within the last 15 years, permanent ice patches in the alpine regions of the Yellowstone area of Montana and Wyoming, Alaska, the southern Yukon, and the western Northwest Territories have been the focus of much study, as they are proving to be a rich source of archaeological information (Kuzyk et al., 1999; Hare et al., 2004, 2012; Andrews et al., 2009, 2012; Lee, 2012; VanderHoek et al., 2012). Caribou herds have used the ice patches as refuge from insects and warm summer temperatures for thousands of years (Kuzyk et al., 1999). Artifacts and organic materials found melting out of the patches have linked caribou to ancient hunters (Farnell et al., 2004). Radiocarbon dating

[1] Department of Geography, University of Calgary, 2500 University Drive NW, Calgary, Alberta T2N 1N4, Canada;
[2] Corresponding author: tmeulendyk@gmail.com
[3] Prince of Wales Northern Heritage Centre, PO Box 1320, Yellowknife, Northwest Territories X1A 2L9, Canada

of artifacts and caribou dung indicates that this relationship has existed for more than 8000 years (Hare et al., 2004). Much effort has been focused on piecing together human history in the region on the basis of finds from the ice patches. Very little research, however, has been done on the composition of the ice patches themselves—specifically, their internal structure, geometry, and development.

The internal structure and geometry of ice patches can be determined using a combination of ground-penetrating radar (GPR) and global positioning system (GPS) techniques (Annan, 2002). In Japan, GPR surveys have taken place on mountainous perennial snow patches since the 1980s (Yoshida et al., 1983). The features termed "snow patches" in Japan have a very similar appearance to the ice patches of the Yukon and Northwest Territories. Located in the Japanese Alps, these snow patches consist of a perennial layer of snow or firn (or both) and an older ice zone, which together are often more than 20 m thick (Sakai et al., 2006). "Firn," in this environment, refers to new snow that has survived a melt season and densified (Anderson and Benson, 1963). Canadian and Japanese patches, however, differ in both age and source of material. The oldest snow patch identified in Japan formed between 1000 years BP and 1700 years BP, according to radiocarbon dates extracted from the lower ice zone (Nakamura, 1990). The bowl-shaped Japanese snow patches develop mainly in glacial cirques and accumulate through avalanching (Higuchi et al., 1980). Ice bodies may form beneath the snow, mainly through the formation of superimposed ice (Kawashima et al., 1993). On the basis of limited research, it appears that ice patches in the Canadian Subarctic develop on bare alpine slopes as snow drifts. The general form and location of the snow accumulations are topographically controlled (Green and Pickering, 2009). An underlying ice body gradually accumulates as the snow and firn densify. Farnell et al. (2004) suggest that the ice body forms through compaction and regelation of melting snow in the summer. Canadian ice patches are maintained by a sensitive balance between accumulation and ablation. GPR surveys of snow patches have revealed several important features, including basal structure, the perennial snow–ice zone contact, and the existence of internal gravel layers (Yamamoto and Yoshida, 1987). Sakai et al. (2006) identified a clear reflection within the snow zone that they suggest is a dirt layer formed from the concentration of annual layers over several years. Reflections within the ice zone were interpreted as gravel layers, which were formed by stones falling from the cirque wall or transported debris flow, or both (Sakai et al., 2006). Some studies used vertical coring of the snow patches to delineate their structure and extract material for dating (Yoshida et al., 1983; Iida et al., 1990; Nakamura, 1990).

Ground-penetrating radar is well suited to ice patch research because radar pulses propagate through ice with little attenuation. Ground-penetrating radar reflections in ice masses are generated by changes in the relative dielectric constant, which is dependent on a variety of physical properties including the orientation of the ice crystal c-axis (Watts and Wright, 1981), the water content, the presence of ionic impurities or air in the ice matrix, and the presence of sediment in the ice (Woodward and Burke, 2007). The relative transparency of ice to radar waves means that considerable depths may be surveyed, providing valuable information on ice thickness, internal structures, the nature of the ice–bed interface, and hydrology (Plewes and Hubbard, 2001). Reflections seen in radar images of the overlying snow and firn can be attributed to differences in density (Paren and Robin, 1975), liquid-water content (Macheret et al., 1993), chemical composition, microparticle concentration (Daniels, 1996), and crystal fabric (Fujita and Mae, 1994). With GPR, ice cores separated from each other by significant distances can be correlated, and the spatial behavior of the stratigraphy can be mapped between the cores (Pälli et al., 2002). Siegert and Hodgkins (2000), for example, traced isochronous internal ice-sheet layering between two core sites 1100 km apart in Antarctica using airborne radar. Ice core data, while limited to the drill site, provide excellent records of past climate and environmental change (Pälli et al., 2002).

This study uses a combination of methods to investigate NWT ice patches. GPR, a non-invasive tool, provides images of their internal architecture. Ice coring is used to ground-truth GPR data and reveals the physical properties (colour, crystallography, etc.) of the ice. Coring also provides organic material preserved within the ice patches, which can be radiocarbon-dated. In combination, radiocarbon dates, GPR data, and ice cores give a better idea of ice patch architecture, ice accumulation, and patch growth. The extracted organic material is used in sister studies to establish regional palaeoenvironmental and palaeoclimatic conditions, as well as caribou dietary and migration patterns (see Galloway et al., 2012; Letts et al., 2012).

The goals of this study were to determine the geometry and internal structure of two NWT ice patches using GPR and ice cores and to construct a conceptual model of ice patch development based on radiocarbon dates of organics cored from the patches.

STUDY AREA

The study area lies in the Mackenzie and Selwyn Mountains between Macmillan Pass (63˚18′ N, 129˚48′ W) and the O'Grady Lake region (62˚59′ N, 129˚05′W) along the east side of the Yukon-NWT border (Fig. 1). Kershaw (1983) describes the region as having a continental climatic regime modified by the alpine environment. According to Wahl et al. (1987), the area experiences mean daily temperature of -7˚C and mean annual precipitation of more than 600 mm. Permafrost is extensive and often continuous throughout the study area (McGinley, 2008).

The Backbone Range of the western Mackenzie Mountains is primarily composed of Silurian and Devonian limestone, dolomite, and calcareous shales, with some

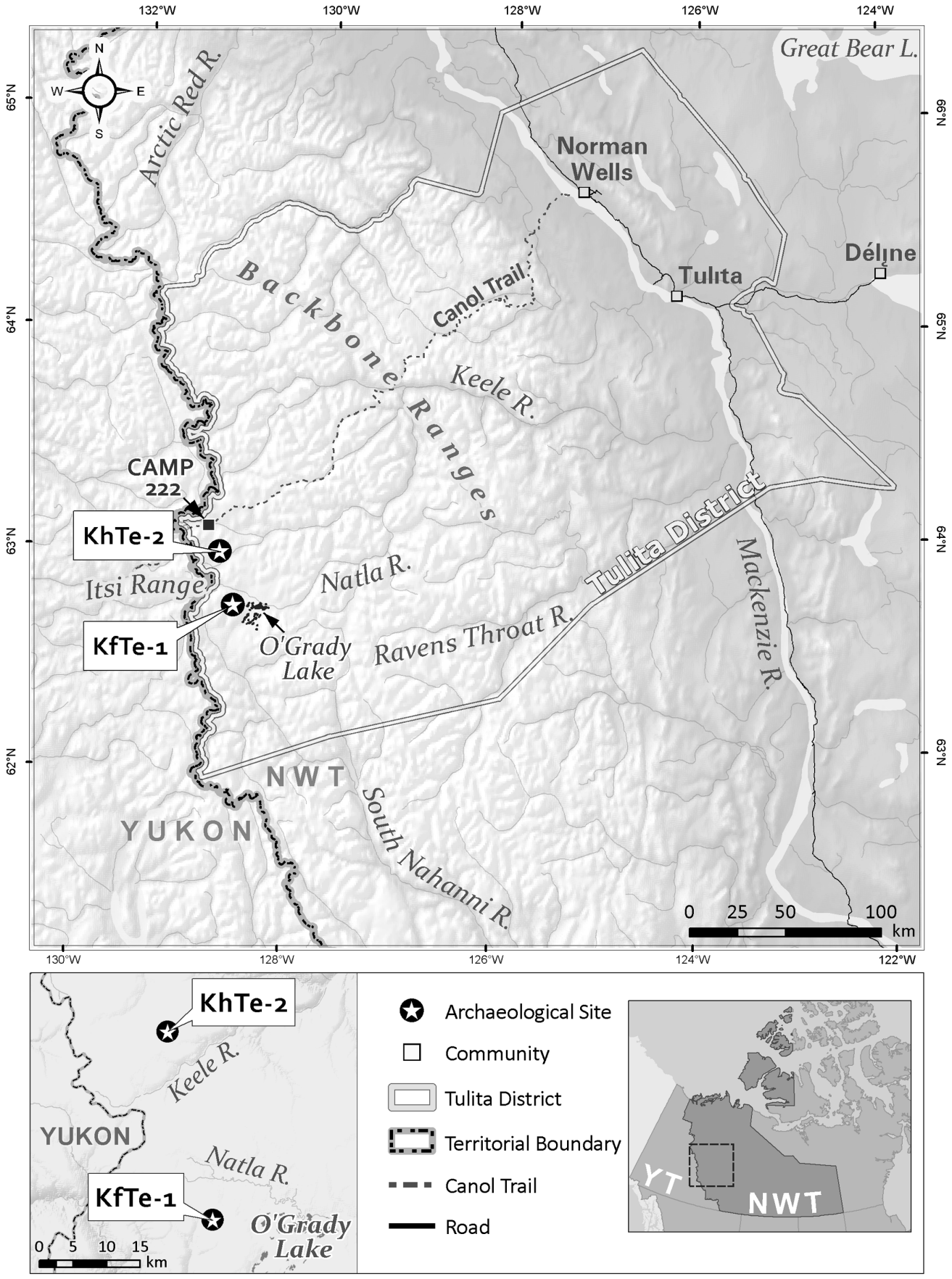

FIG. 1. Locations of the two ice patches under study, KfTe-1 and KhTe-2, in the Mackenzie and Selwyn Mountains.

Precambrian quartzites (Aitken and Cook, 1974; Szeicz et al., 1995). Immediately west of the Backbone Range lies the Itsi Range of the Selwyn Mountains. These mountains are composed of Paleozoic clastics and Mesozoic intrusive. In the surrounding basins, considerable amounts of Quaternary glacial and alluvial deposits overlie the Paleozoic clastics (Blusson, 1971).

The detailed glacial history of the area is poorly understood (MacDonald, 1983). Mountain summits rising above 2500 m have been intensely eroded by glacial action and sculpted into alpine cirque, arête, and horn topography (Jackson et al., 1991). Lower peaks were overrun by glacial ice, which produced their present-day domed summits. Beginning in the Late Pliocene and continuing through the Pleistocene, all glaciations of the Mackenzie and Selwyn Mountains featured a cordilleran ice sheet on the western side of the continental divide and valley glaciers on the eastern side (Duk-Rodkin et al., 1996). The latest glaciation took place during the Late Wisconsinan (Klassen, 1987; Jackson et al., 1991). The advance of Cordilleran ice or large montane glaciers, or both, over the study area is locally termed the Gayna River Glaciation. This event corresponds to the McConnell phase in the Yukon, which reached its peak less than 23 000 years ago (Szeicz et al., 1995). Deglaciation of the region was complete by 10 000 years BP. However, a few locally extensive cirque glacier complexes remain, and ice fields exist in the Itsi and Ragged ranges of the Selwyn Mountains above 1900 m. Their descending valley glaciers reach as low as 1500 m (Jackson et al., 1991).

Perennial alpine ice patches exist within the study area between 1600 and 2000 m elevation. This research focuses on two ice patches (KfTe-1 and KhTe-2) within the study area where members of the NWT Ice Patch Study identified archaeological remains in previous years.

KfTe-1 (62˚58′ N, 129˚20′ W) faces north-northeast and rests on a leeward slope at an elevation of 1744 m (Fig. 2). In 2008, the ice patch was approximately 192 m long and 39 m wide at its widest point. It consists of a large ice body overlain by firn and snow, the lower portion of which is characterized by a steep face, 2 – 3 m high. The face reveals some of the internal stratigraphy of the ice patch. Snow cover has an average slope angle of 30˚ from vertical. Caribou dung surrounds all margins of KfTe-1. Narrow meltwater streams descend from the lower margin of the patch over the fractured shale bedrock.

KhTe-2 (63˚11′ N, 129˚37′ W) lies 28 km northwest of KfTe-1 on a similar northeast-facing leeward slope. At an elevation of 1850 m, the ice patch was 230 m long and more than 25 m wide in 2008. KhTe-2 also has a steep lower portion and an average slope angle of 27˚. The ring of dung surrounding this ice patch is 5 – 10 m wider at the upper margin than the one at KfTe-1. Longitudinal furrows (possibly caribou tracks) in the snow cover are present. Caribou tracks migrating away from the margins of the ice patch are present on the surrounding fractured shale slopes.

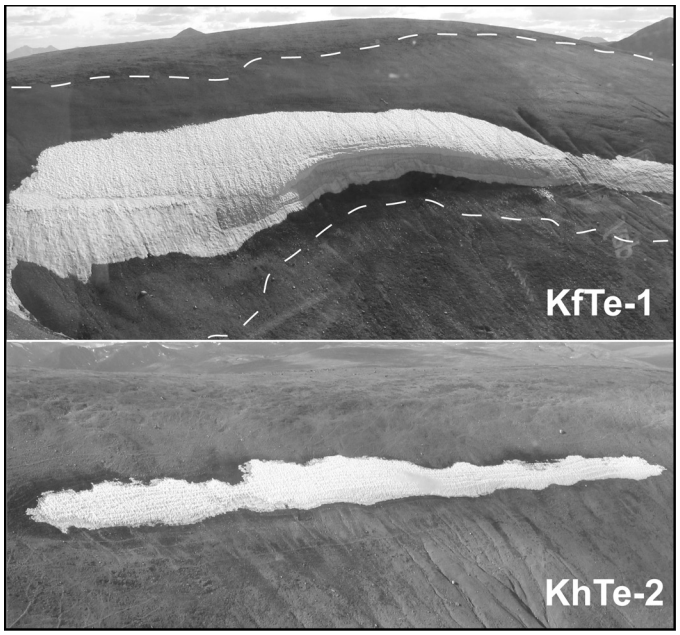

FIG. 2. Study sites KfTe-1 and KhTe-2 viewed from the east. Note the unvegetated slope (area between dashed lines) around KfTe-1, which indicates former ice patch extent.

METHODS

GPR System and Survey Parameters

An investigative field season was completed in 2007 (14 – 17 August) at sites KfTe-1 and KhTe-2 using 200 MHz and 500 MHz Noggin GPR systems. When used in combination, the 200 MHz and 500 MHz antennae were separated by 165 cm (Fig. 3). Data were recorded using a Digital Video Logger (DVL). A Garmin GPSMAP 76S unit was connected directly to the DVL to record positional data. Based on the 2007 field investigation, data were collected using only the 500 MHz Noggin system during the more extensive 2008 field season (11 – 17 August). The furrowed snow surfaces of KfTe-1 and KhTe-2 occasionally caused the antenna to tip and lose contact with the surface. While rare, these occurrences negatively affected the quality of data for a very short period. The antenna was fitted with an outrigger to prevent tipping and roll-over (Fig. 3B).

Ground-penetrating radar data were continuously sampled in free-run mode with a time window of 132 ns. Data stacking, which improves data quality by averaging multiple traces at each survey position, was set to 4 as there was very little external electromagnetic (EM) noise in this remote area. A Garmin eTrex GPS unit was linked to the Noggin system, which took a GPS coordinate for every five traces collected. While recording locations, the Garmin eTrex was fastened approximately 1.5 m above the ground surface. The coordinates allowed for positioning of each transect, and future distance and step-size correction (typical error was ± 8 m, as quoted by the GPS). Erroneous GPR coordinates were corrected using surrounding, higher accuracy coordinates. In addition, the GPS unit was used

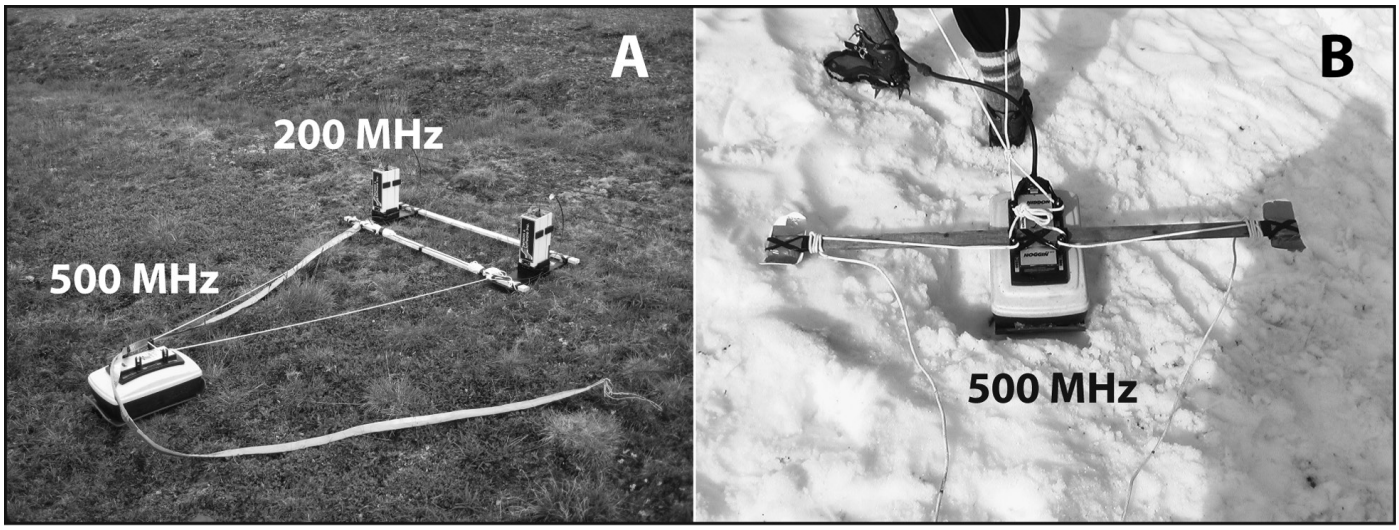

FIG. 3. (A) The 200 MHz (separate antennas) and 500 MHz GPR configuration during the 2007 field season and (B) the outrigger fastened to the 500 MHz antenna used in 2008.

to map the margins and snow extent of KfTe-1 and KhTe-2 during the end of the ablation period over a three-year span (August 2007–09).

In 2007, 18 transverse lines (transects) of GPR data were collected in a zigzag manner over the thickest area of the KfTe-1 ice patch (Fig. 4). A thin section of annual snow to the northwest was not surveyed. The Garmin unit attached a GPS coordinate to every fifth trace collected by the 200 MHz antenna. In 2008, we collected data from 20 transects in a very similar zigzag pattern. To increase spatial coverage, data were also collected longitudinally across the patch. These 30 surveys were conducted at a constant, swift walking pace with a typical trace spacing of 2.5 cm.

On the much narrower KhTe-2 ice patch, we collected data along 31 transverse transects in 2007. Each line started and finished at the ice margin. Only the 500 MHz antenna was used during this survey because this antenna had been found to be optimal during surveys at KfTe-1. Collecting data in a zigzag pattern allowed for sufficient spatial coverage. Each transect represents a complete ice patch cross-section at its respective location. In 2008, 42 transects were again collected in a zigzag manner. A single longitudinal line was run from the SE end of the patch to the NW to increase spatial coverage (Fig. 4). The lower surface of KhTe-2 was quite steep across much of the patch. Consequently, the operators were able to reach the lower margin with the antenna only on the gentler, NW portion. The remaining zigzag transects were run from the upper margin of the ice patch to the ridge of the sheer section. The pacing was less constant on some of the steep, furrowed sections of KhTe-2; as a result, the trace spacing ranges from 1 to 5 cm.

GPR Data Processing and Interpretation

The initial stages of GPR data processing were completed on all transects collected in 2007 and 2008 using the following software: REFLEXW and WIN EKKO PRO. Dead traces, which are repeated duplicates imaged when the antenna is motionless, were removed from each profile. Due to signal attenuation, some profiles contained weaker reflections at depth. An automatic gain control (AGC) of 30 with a window width of three pulses was used to enhance weaker reflections. Profiles were also "de-wowed" to remove low-frequency noise. Data migration was applied to some profiles, but was not found to improve data quality significantly for all lines. Trace spacing and transect length needed to be corrected as the antennae were not always dragged at a constant pace, particularly on steep slopes. Following these steps, the positions of the most coherent, continuous reflections were recorded through a process known as "picking." During this process, the depth (two-way travel time) was taken or "picked" every 2 m along the length of each reflection for all profiles. For each continuous reflection, the uppermost peak phase (typically positive) was picked.

Using the lengths of ice cores extracted from both patches, a general depth axis was constructed for all profiles (Fig. 4), with a velocity of 0.18 m/ns. Across both ice patches, the ratio of ice thickness to snow depth was found to be approximately 3:1. Published propagation velocities for ice (0.17 m/s; Annan, 2001) and snow (0.22 m/ns; Galley et al., 2009) suggest that the weighted velocity (0.18 m/ns) is appropriate.

Combining average velocity with pulse period (inverse of the antennae frequency) provides an excellent estimation of pulse wavelength. Assuming that theoretical vertical resolution is one-quarter of the wavelength, the resolution is estimated to be 0.09 m and 0.23 m for the 500 MHz and 200 MHz antennae, respectively. This allows for excellent imaging of the gross structure of the ice patches and internal layers thicker than 9 cm.

Errors within the GPS elevation values made the topographic correction of the GPR profiles impossible. Consequently, ice patch surfaces were interpreted as flat, and

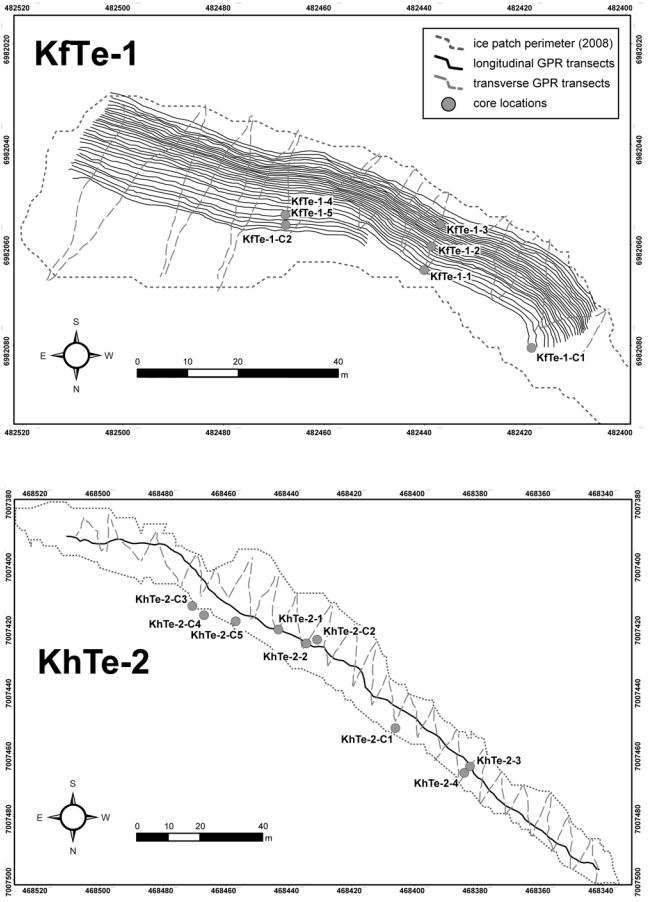

FIG. 4. Maps of KfTe-1 and KhTe-2, showing the locations of GPR transects and cores collected during the 2007 and 2008 field seasons.

subsurface GPR reflections are not in their true orientation. However, other than a general dip from the upslope margin to the downslope margin of both ice patches, there is not a great deal of relief change across the patches (i.e., along longitudinal GPR profiles), and therefore the "true" geometry of the subsurface reflections is not far from those presented.

Ice Coring Parameters

During both field seasons, ice cores were drilled and extracted using a Cold Regions Research and Engineering Laboratory (CRREL) coring auger. The cores were approximately 7.5 cm in diameter and 20–320 cm in length. The ice patches were cored at approximately true vertical, rather than perpendicular to the surface dip. Coring locations were chosen strategically on the basis of positions of GPR lines and characteristics observed in the raw GPR profiles (i.e., many reflections; Fig. 4). The core locations were numbered sequentially, and the GPS coordinates of each were collected using a Garmin eTrex. Recording took place while the unit was held approximately 1 m above the ground surface with an error of ± 6 m (as quoted by the GPS unit). In 2007, two cores were extracted from KfTe-1 (KfTe-1-C1, KfTe-1-C2) and five from KhTe-2 (KhTe-2-C1, KhTe-2-C2, KhTe-2-C3, KhTe-2-C4, KhTe-2-C5). In 2008, KfTe-1 was initially cored in four locations. However, the coring barrel became lodged during the removal of core KfTe-1-4, so an adjacent fifth core was extracted (KfTe-1-5). The partially extracted KfTe-1-4 and complete KfTe-1-5 cores were frozen to a colder temperature and shipped to the University of Calgary for further analysis. Four cores were removed from KhTe-2. Each core was extracted, described, photographed, and videotaped for further study. Dung pellets or lenses identified in any of the cores were preserved for dating and analysis purposes. Dung layers from four KfTe-1 ice cores (KfTe-1-C1, KfTe-1-C2, KfTe-1-4, KfTe-1-5) and five KhTe-2 cores (KhTe-2-C1 to KhTe-2-C5) were radiocarbon-dated (see Table 1 in Galloway et al., 2012). Radiocarbon dates were calibrated using CALIB6.0 (Stuiver et al., 2005) and the INTCAL09 dataset (Reimer et al., 2009).

Measurement of Ice Properties

As stated, physical and chemical changes within the subsurface can affect the EM properties and therefore the radar response. To determine what changes are producing reflections within the GPR profiles, a preserved ice core was analyzed. Unfortunately, because of logistical constraints, measurements of electrical conductivity or liquid water content could not be undertaken in the field, and the field conditions could not be replicated in the laboratory. Instead, measurements of liquid conductivity, pH, and mass of incorporated material were taken along the length of the core. Correlating the profiles of these properties with the radar response where the core was extracted will show any relationships.

The partially recovered core KfTe-1-4 was cut transversely into 4 cm sections, which were then melted in individual containers. Once the samples reached room temperature (~22˚C), the liquid conductivity and pH were determined using an Accumet AP85 portable pH/conductivity meter. A vacuum method was used to isolate all the incorporated debris (i.e., sediment and organic material) from the liquid. The debris was dried and weighed. Recorded measurements were compiled into profiles for each property. The dry mass of each dung pellet removed from KfTe -1-4 during the 2008 field season was added to the profile of incorporated material at the appropriate depths.

RESULTS AND INTERPRETATION

Ice Core Data

The patches of ice under study, KfTe-1 and KhTe-2, were overlain by snow and firn. At KfTe-1, coring revealed that snow cover was typically 50 to 100 cm thick in 2007 and 2008, though in one area, snow and firn reached a depth of over 2 m (Fig. 5). The transition from snow to firn was sharp in some cores and more gradational in others. At KhTe-2, snow cover was generally thinner (< 70 cm) in 2007 and 2008, and firn was absent from all core sites. The snow

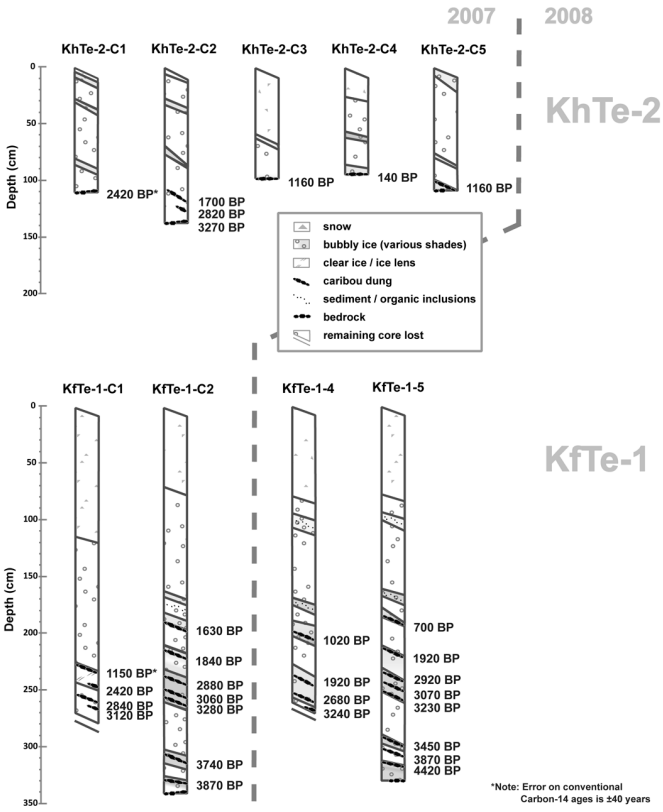

FIG. 5. Logs of ice cores collected at KhTe-2 and KfTe-1 in 2007 and 2008 that contained radiocarbon-dated dung layers.

and firn were found to contain a high amount of unfrozen water at all core sites, as well as occasional ice lenses. Over the study area, the snow and firn colour is fairly constant. However, at KhTe-2, fresh deposits of caribou dung were found to alter the colour of snow a few centimetres below the surface in 2007. In some cores, thin layers of fine sediment or organic inclusions were identified within the snow. At KfTe-1, some thin ice lenses were found within the firn layer.

The transition from snow/firn to ice was easily identified at all core sites where firn was present (Fig. 5). At the snow-ice contact, the first 5–10 cm of ice occasionally had a brown or gray colour and contained some organic sediment. A similar colour was present in the upper layer of ice (< 10 cm) at KhTe-2 in places where snow cover was absent. Each core showed that the ice is composed of distinct strata that have a consistent frequency of bubbles throughout. These bubbles are predominantly spherical (1–6 mm in diameter), though elongate bubbles (up to 20 mm long) with a subhorizontal orientation (relative to true horizontal) were also identified.

An assessment of ice crystallography shows that crystals are equidimensional (up to 5 mm in diameter), with no preferred orientation. Bubbles are found within crystals and at crystal boundaries. Thin layers of bubble-free ice were identified in two KfTe-1 cores. Some sections of bubbly ice contained bands of fine sediment or organic inclusions, in both continuous and discontinuous bands.

Thick deposits of organic material, identified as caribou dung, were found in nearly all cores taken from both study sites (Fig. 5). The continuous and discontinuous dung bands, sometimes containing intact pellets, were between 0.2 cm and 7 cm thick; they were often surrounded by thick layers of coloured ice—usually yellow, green or gray (Fig. 6). Yellow and green ice contained dung particles, while the presence of sediment and fine organic matter gave ice a gray appearance. Periodically, coloured ice layers were found unaccompanied by dung, and colourless ice layers containing dung were also found. The dip angle for each layer within the ice varied between 10˚ and 45˚ from horizontal and differed from the surface dip by up to 30˚. All cores except two terminated at the base of the ice. The basal ice often contained discontinuous dung layers or entrained bedrock.

GPR Results

Ground-penetrating radar surveys at KfTe-1 and KhTe-2 display a number of recurring, continuous reflections (Figs. 7–9), though the air wave and ground wave mask the upper 20–30 cm of the profiles. Through the correlation of GPR profiles and ice cores, it is possible to verify the sources of the continuous reflections. Between 0 ns and 15 ns in all profiles, a strong reflection is present that becomes shallow or non-existent at the ice patch margins. This reflection coincides with the snow/ice or snow/firn contact and is dominantly a function of the change in air content, but also of the increased liquid water content at this interface. In some radar profiles taken from core locations, reflections in the snow, firn, and ice layers do not correspond to observable changes in the cores. The bottommost reflection is continuous through the patches, and only weak returns and noise are identified below it. This reflection correlates with the ice/bedrock contact because its depth at both ice patches corresponds with the termination points of each ice core (except those holes that were abandoned). The significant change in the dielectric constant between ice and the underlying shale generates a strong reflection.

The reflections between the snow/ice or firn/ice contact and the bedrock reflection at KfTe-1 and KhTe-2 are multiple reflections that are continuous (uninterrupted) through the profile (Figs. 7 and 9). These reflections correlate to the presence of dung concentrations and layers of organic particles and sediment in the ice cores (Fig. 7). The uninterrupted nature of intra-ice reflections indicates dung layers are continuous rather than localized deposits. However, some of the ice cores contain a number of dung bands that do not produce distinct reflections. For example, core KfTe-1-5 contains eight intra-ice dung bands yet the radar profile has only four or five correlating continuous reflections. The reason is that the small separation of some dung bands is less than the vertical resolution of the 500 MHz radar. These closely spaced multiple dung bands combine to produce single reflections in the GPR profiles. In addition to strong reflections associated with dung, a number of weaker

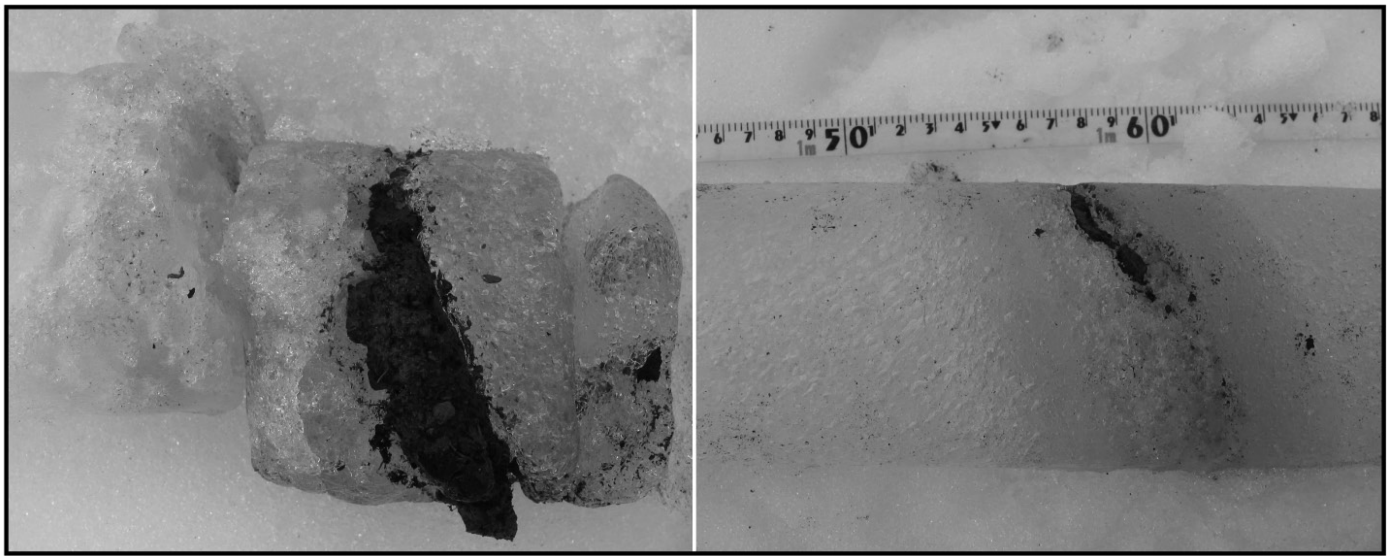

FIG. 6. Examples of dung bands found in the ice cores. The several centimetres of darkened ice around these dung lenses correspond to coloured ice found in conjunction with dung and sediment bands.

continuous reflections match with thin layers of organic and inorganic coarse sediment or wider layers of gray/brown ice containing fine sediment. Furthermore, coloured ice layers (yellow and green) produce noticeable reflection events within KhTe-2 even where dung is not present.

Bulk conductivity and pH measured along the length of the ice section of core KfTe-1-4 appear to have little effect on the GPR response, though there are some exceptions (Fig. 8). Peak values for both properties at 250 cm depth correlate with high reflection amplitudes in the radar response at 27 ns, but this correlation is likely due to the fact that the samples measured were unfiltered. The melted section of ice at 250 cm depth contained a significant amount of suspended caribou dung, which could have affected the instruments. While the bulk conductivity profile does contain smaller peaks, nearly all measured values are low (< 25 µS). These results are expected, as the low-conductive environment contributes to the ability of GPR to image the entire ice patch structure.

Along the length of the ice core, pH values are between 5 and 8. A slight jump in pH between 185 cm and 200 cm depth correlates with a band of coloured ice (particulate dung) in the ice core and higher amplitudes in the response of the 500 MHz radar.

Figure 8 shows that the amount of incorporated sediments and organic material has the greatest visual correlation with the 500 MHz radar response. High reflection amplitudes in the ice section (21 ns and 27 ns) correspond to peak values of incorporated organics (i.e., dung layers at 190 cm and 245 cm depth). Even a layer of relatively low sediment/organic mass (95 cm depth) appears to produce a response. The 95 cm deep layer relates to a high-amplitude return while a deeper sediment layer (225 cm depth) does not. The two layers have similar amounts of incorporated sediment (< 5 g), but the 225 cm layer is only 6 cm thick, which is below the vertical resolution of the GPR unit in this environment, and therefore its reflection would not appear in the profile. Two coloured ice bands in KfTe-1-4 associated with the dung layers, while in no way measured, also visually correlate with the high-amplitude returns. The relationship between high amplitude radar response and caribou dung and particles holds true at all core locations.

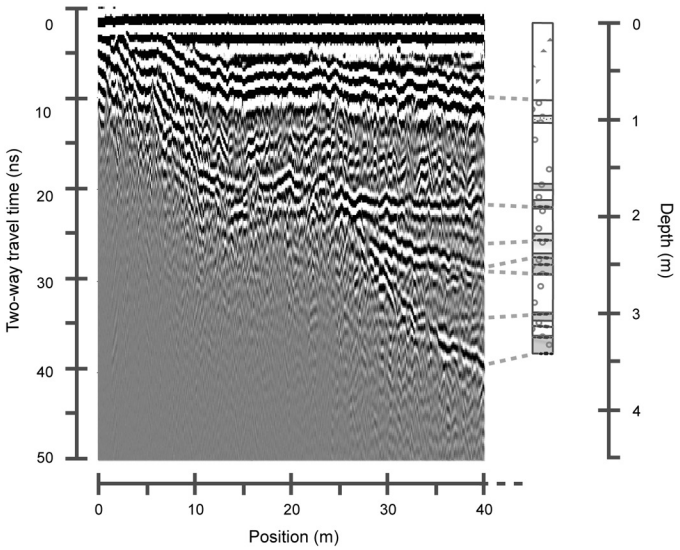

FIG. 7. The correlation of a 500-MHz GPR profile section from KfTe-1 and ice core log KfTe-1-5, showing reflection events attributed to the presence of dung layers within the ice. Other strong reflectors correlate with the snow-ice contact and the base of the ice patch.

Ice Patch Architecture

Ground-penetrating radar profiles collected at KfTe-1 during the end of an ablation period (August 2008) show that snow cover reaches depths of more than 1 m (Fig. 9). The base of the snow layer is saturated by unfrozen water. A separate area of water-saturated firn, up to 1.5 m thick,

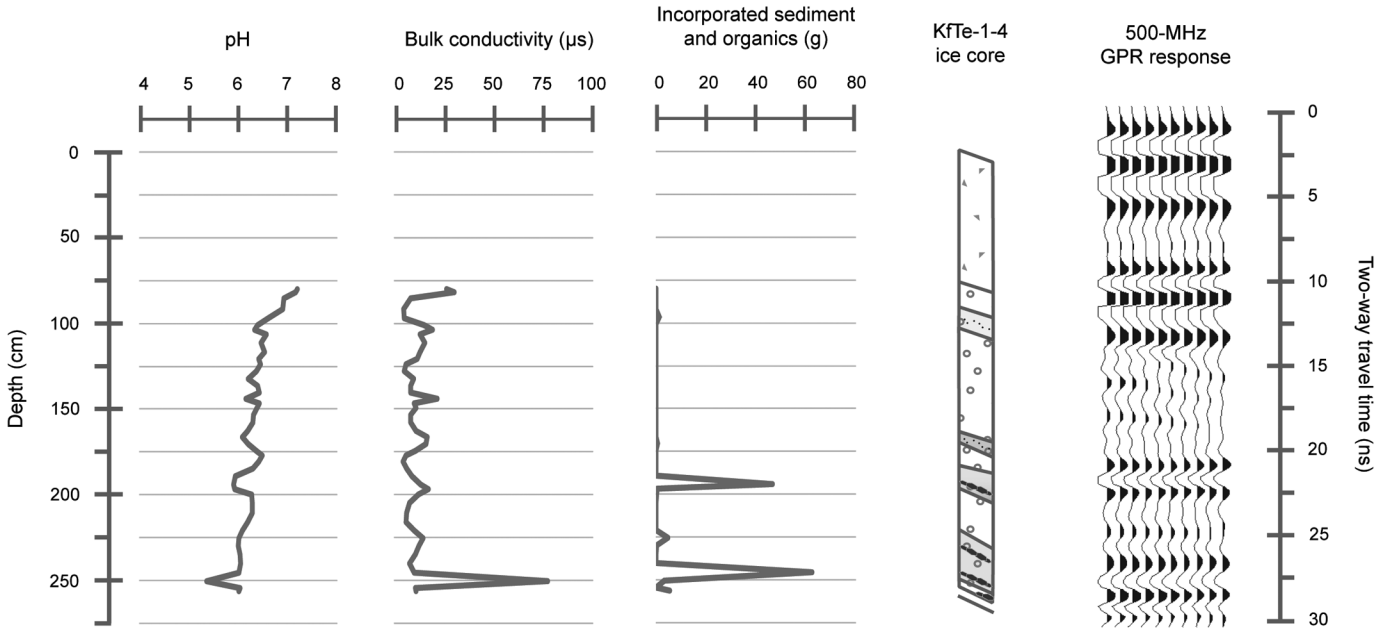

FIG. 8. Measurements of pH, bulk conductivity, and incorporated sediment and organics from the ice section of core KfTe-1-4 compared to the response of the 500 MHz GPR unit at the core location. Peak masses of incorporated sediment and organic matter correlate with high-amplitude values in the GPR response.

is also present. At its thickest point (10 – 17 m from the upslope margin), KfTe-1 contains between three and seven distinct ice bodies separated by continuous layers of caribou dung, dung particles, and sediment. As the GPR profiles show, most ice bodies have limited horizontal extent, and the dung layers merge at their margins. The limited size of the individual bodies gives the ice core a staggered or offset structure and makes it difficult to discern their depositional ordering (Fig. 10). The uppermost ice body is spatially continuous to the ice patch margins and is underlain by relatively older, smaller ice bodies in the thickest area of the ice patch. The ice patch rests in a longitudinal trough in the shale slope, which is likely a nivation hollow that forms through the weathering and transport by meltwater of fractured shale from beneath the ice patch.

Ground-penetrating radar profiles show that KhTe-2 has a fairly uniform thickness throughout (Fig. 9). Snow cover is up to 1 m thick late into the ablation period and extends beyond the margins of the underlying ice core. The core of ice has a maximum thickness of 1.2 m and is composed of three distinct bodies, which have a staggered or offset orientation (Fig. 11). As in KfTe-1, the uppermost ice body has the greatest spatial extent. However, in contrast to KfTe-1, where the intra-ice dung layers appear to be continuous, KhTe-2 ice bodies are separated by discontinuous dung concentrations. In the absence of dung, bands of sediment and dung particles mark the contacts between the ice bodies.

Distribution of Snow Accumulation

Between individual years of study the snow extent changed quite dramatically for KfTe-1, but the net change over the three-year period was minimal (Fig. 12). The loss in total snow extent from 2007 to 2008 was approximately 5292 m^2. The large impacted area to the northwest was predominately snow, though some sections were underlain by thin ice. Overall, KhTe-2 snow extent gradually decreased over the recorded period. Between 2007 and 2008, the northwest end of KhTe-2 expanded and developed nearly 30 vertical centimetres of new ice, according to GPR profiles. However, some sections of ice up to 50 cm thick were lost at the northeast (downslope) margin after 2007, whereas the upslope margin changed very little.

Whilst KfTe-1 displays more drastic changes in snow extent, both ice patches experienced a net decrease in total area over the recorded period. From 2008 to 2009, snow extent more than doubled at KfTe-1, but diminished by 25% at KhTe-2. Given that the patches (less than 30 km apart) experienced nearly identical climatic conditions during this study, the discrepancy in snow accumulation/ablation suggests that annual snow extent is controlled by factors other than simply precipitation and temperature.

Temporal Record

Radiocarbon dates are summarized in Figure 5. The oldest dung layer found at KfTe-1 is 4420 ± 40 ^{14}C yr BP (ca. 5070 ± 200 cal. yr BP). At KhTe-2, the oldest recorded layer is 3270 ± 40 ^{14}C yr BP (ca. 3500 ± 110 cal. yr BP). Dates from basal dung were collected from five ice cores (KfTe-1-C1, KhTe-2-C1 to KhTe 2-C4). Radiocarbon dates of dung cored from the base of ice patches are considered inaccurate indicators for the age of overlying ice. After basal dung was deposited, the amount of time that passed before it was covered by snow and ice is unknown. For example, ice cores KhTe-2-C3 and KhTe-2-C4, extracted near the periphery of KhTe-2 in 2007, provided basal dung dated at 1160 ± 40 ^{14}C

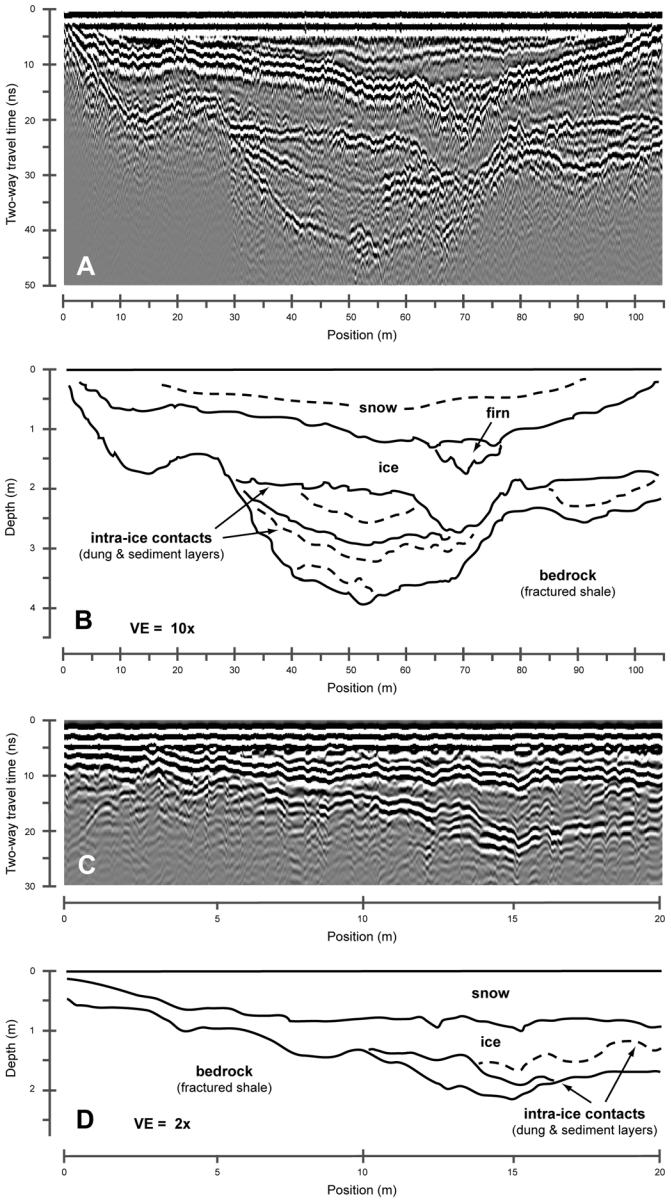

FIG. 9. (A) A 500 MHz GPR profile from KfTe-1 and (B) its corresponding interpretation. (C) A 500 MHz GPR profile from KhTe-2 and (D) its corresponding interpretation. The dashed lines represent weaker reflections.

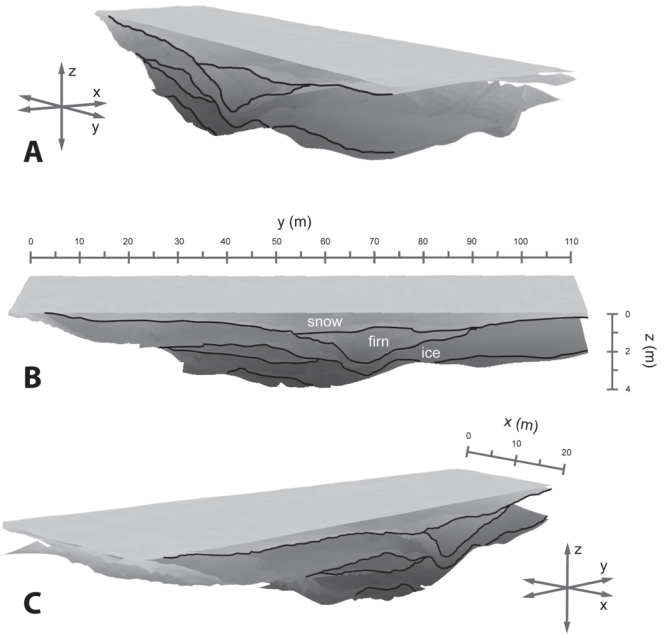

FIG. 10. A three-dimensional construction of KfTe-1 based on GPR interpretations, which shows the contacts between the snow, firn, and ice zones, as well as the most prominent intra-ice layers. Viewed from the (A) north-northwest, (B) northeast and (C) east.

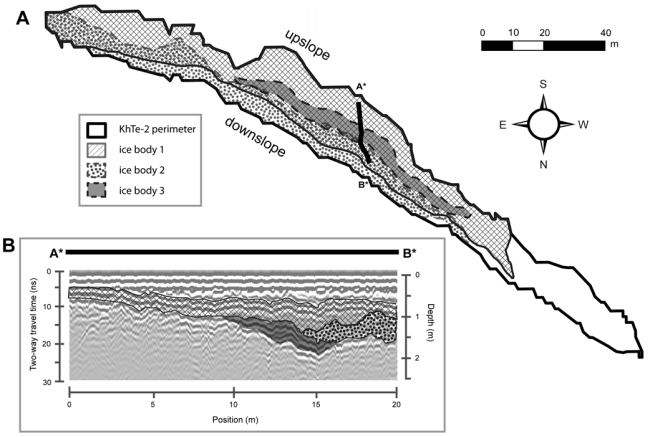

FIG. 11. (A) Planar view of KhTe-2, showing the extent of its individual ice bodies and the location of (B) a GPR profile revealing the cross-sectional orientation of the ice bodies.

yr BP (ca. 1070 ± 100 cal. yr BP) and 140 ± 40 ^{14}C yr BP (ca. 140 ± 140 cal. yr BP), respectively. Basal dung and intra-ice dung extracted upslope from these sites was considerably older. In addition, the KhTe-2-C3 and KhTe-2-C4 core locations were no longer present in 2008, as the ice patch margin had retreated upslope. This retreat suggests that the ice at the margins is ephemeral.

With the aid of GPR profiles, it is possible to correlate dung layers between ice cores. Figure 13 shows cores KfTe-1-C2, KfTe-1-4, and KfTe-1-5, which were collected in close proximity. As expected, the general stratigraphy of the cores and the depths associated with the dung layers are similar. The uppermost dung layer provides dates of 700 ± 40 ^{14}C yr BP (ca. 640 ± 80 cal. yr BP), 1020 ± 40 ^{14}C yr BP (ca. 930 ± 130 cal. yr BP), and 1630 ± 40 ^{14}C yr BP (ca. 1550 ± 140 cal. yr BP), showing a 930-year gap between the earliest and latest conventional dates measured at that horizon. This pattern is present to varying degrees at each dung layer, indicating that long periods of time may pass before there is a net accumulation of overlying snow and ice.

An average rate of accumulation for the individual ice bodies can be determined using the radiocarbon dates gathered from each dung layer. For each ice body, the vertical thickness is divided by the difference between the radiocarbon dates of the over- and underlying dung layers (Fig. 14). The average accumulation rate applies to the period of time between the dated dung layers (i.e., from 1630 years BP to the present, the ice of KfTe-1-5 accumulated at an average rate of 0.074 cm/year). The uppermost ice body of each core

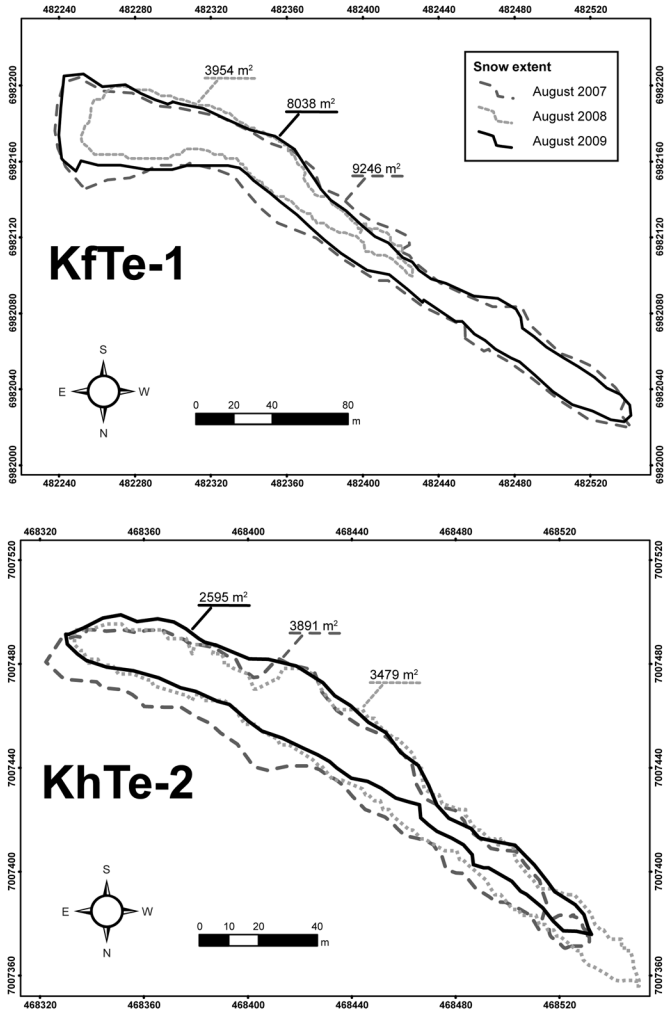

FIG. 12. Maps of KfTe-1 and KhTe-2, showing the approximate total areas of snow extent late in the ablation season (mid-August) over a three-year period (2007 to 2009).

has a surface date of 0 years BP as it is covered in snow from the previous winter. It should be noted that the annual accumulation rate of ice is thought to vary dramatically. Because of their inaccuracies, described above, basal radiocarbon dates are not used when determining average accumulation rate.

At KfTe-1, the average accumulation rate was calculated for the ice bodies of cores KfTe-1-C2, KfTe-1-4, and KfTe-1-5. All three cores show an overall increase in average accumulation rate for the last 3000 years. KfTe-1-5 and KfTe-1-C2 exhibit an earlier significant decline in accumulation rates, from up to 0.186 cm/year, between 3500 years BP and 3000 years BP.

Only two cores from the second ice patch (KhTe-2-C2 and KhTe-2-C5) could be used to calculate average accumulation rate after basal dates were excluded. Between 2820 and 1700 years BP, ice from KhTe-2-C2 accumulated at an average rate of 0.012 cm/year. From 1700 years BP to the present, the rate increased to 0.060 cm/year. Ice from KhTe-2-C5 accumulated at an average rate of 0.084 cm/year between 1160 years BP and the present.

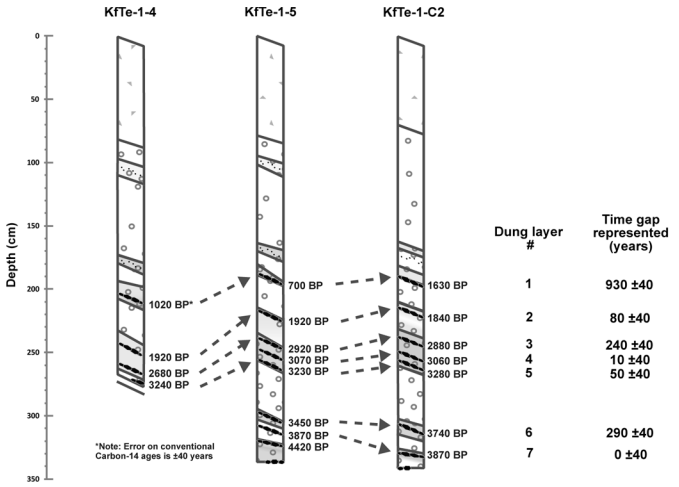

FIG. 13. Correlation of dung layers between three ice cores from KfTe-1 and the gaps in time represented. Dates are radiocarbon years before present.

DISCUSSION

NWT Ice Patch Development

Extant glacial ice and ice fields still exist in the region at an elevation range similar to that of NWT ice patches (Jackson et al., 1991); however, basal radiocarbon dates from both patches suggest that these ice patches formed during the Holocene rather than being glacial remnants. From the thickest area of KhTe-2, 3270-year-old dung was extracted, indicating that ice did not exist in that location prior to the mid-Holocene. At KfTe-1, no dung was found to be older than 4420 ± 40 ^{14}C yr BP (ca. 5070 ± 200 cal. yr BP). Throughout the extracted cores, the ice is bubbly, contains small crystals, and lacks any sign of internal deformation, irregular crystals, or any other characteristic typical of glacial ice.

Instead, ice patches initially form as snow drifts (seasonal snow patches) on leeward alpine slopes in the NWT. Winter weather (precipitation, wind speed, and direction) affects the annual variation in morphology of snow patches, while topography influences their general form and location on a longer term (Billings and Bliss, 1959; Hejcman et al., 2006; Green and Pickering, 2009). KfTe-1 and KhTe-2 are found on north-northeasterly facing slopes in an area of southwesterly prevailing winds. A similar leeward snow drifting pattern is seen in snow patch distribution elsewhere (Watson et al., 1994; Davis, 1998). Shallow troughs form beneath perennial patches through the process of nivation, in which mechanical weathering, erosion, and mass movement of fractured shale by meltwater flow create hollows (Berrisford, 1991). Nivation hollows, as displayed in the GPR results, further protect the snow patches and promote increased accumulation of drifting snow. Similar snow extent at KfTe-1 in 2007 and 2009 supports topographically controlled snow drifting. Nivation hollows are also a common feature of ice patches in the southern Yukon (Washburn, 1979; Farnell et al., 2004).

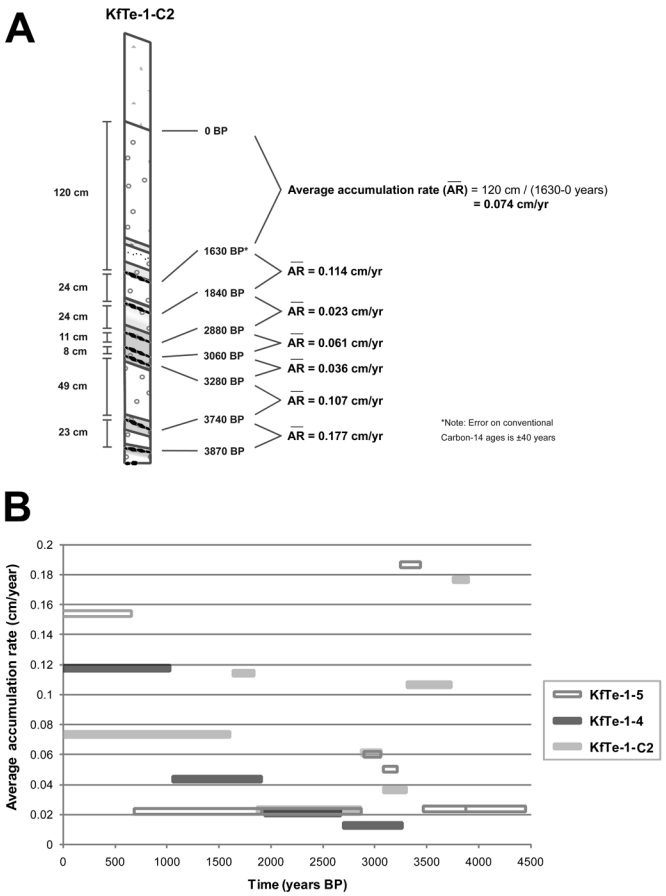

FIG. 14. (A) An example of how average accumulation rate is calculated for individual ice bodies from each core using radiocarbon dates. (B) Average accumulation rates of ice at KfTe-1 during the Holocene based on three ice cores. Dates are radiocarbon years before present.

New snow that is not lost during the ablation season is densified by grain packing. During densification, meltwater percolates through the remaining snow and firn, where it refreezes within the matrix, in a process similar to superimposed ice formation (Kawashima et al., 1993). For situations where meltwater refreezing is prevalent, as we see in NWT ice patches, it dominates the densification process (Cuffey and Paterson, 2010).

Meltwater that is not lost to downslope drainage is held in some pore space of the firn layer by surface tension. In the winter, this water freezes, and pore space is lost within the snow pack. As this process is repeated each year, new snow melts in the summer and the meltwater fills the remaining pores. Consequently, pore size is reduced each year until only isolated air pockets remain and the transformation to bubbly ice is complete.

On KfTe-1 during the 2008 ablation season, the firn layer found beneath new snow was limited to a 1.5 m depression in the surface of the ice core. This fact suggests that firn formation is localized when much of the previous winter's snow was lost. Here, local meltwater flows into this depression, saturating the firn layer. Similar localized firn development has been found at temperate glaciers worldwide (Sharp, 1951; Vallon et al., 1976; Ren et al., 1995). The resulting thickness of the water-saturated firn layer is dependent on the ablation rate, firn permeability, inclination of the firn-ice interface, and the size of the depression (Kawashima, 1997). In the GPR profiles, the presence of water at the base of the firn/ice layer results in a strong and continuous reflection. Prior to ice development, the presence of a water-saturated firn layer at the bedrock contact would accelerate densification and result in a swift transformation from firn to ice (Ogasahara, 1964; Wakahama and Narita, 1975). As saturated firn layers occur in localized depressions, new ice bodies develop in topographic low points on a pre-existing ice body or in between that body and the bedrock. This scenario likely explains why ice bodies in NWT ice patches have a staggered or offset configuration, as displayed by GPR surveys.

Kawashima et al. (1993) found that superimposed ice formation was a significant contributor to the growth of an ice body in ice-cored snow patches in the Japanese Alps (up to 30 cm). While ice lenses found in the firn layer at KfTe-1 are thought to be superimposed ice, the limited numbers of these ice lenses (0.5–1 cm thick) formed at or near the firn base suggest they are not laterally extensive. Indeed, superimposed ice did not correlate with returns in GPR surveys. A possible explanation is that the reflections from the layers and ice lenses merge into a single return and show up as point reflectors or clear layering (Pälli et al., 2003). This conclusion suggests that superimposed ice is not significant in NWT ice patches.

Ice body accumulation does not occur every year on NWT ice patches. Results show that firn at KfTe-1 is restricted to a relatively small area, and it is completely absent at KhTe-2. The remaining area is covered in snow from the previous winter that will be lost during the ablation season. The data from 2007–09 indicate that firn layer formation during that period was atypical for NWT ice patches.

As caribou congregate annually on the ice patches, dung is continually deposited on the snow surface. During these accumulation periods, deposits of dung are preserved beneath the freshly fallen snow as it turns to ice. Ice growth is interrupted by warmer summers resulting in catastrophic melt of the upper ice body. Multiple deposits and layers of caribou dung that were in the lost ice are now concentrated into a single layer. Radiocarbon dates reveal that concentrated dung layers contain organic material deposited over centuries or decades; they record times of no net ice accumulation. Intact pellets, showing minimal signs of weathering, are found in extracted ice cores, indicating that the dung is exposed on the surface for only a short time. Farnell et al. (2004) describe a similar process for the development of dung "super layers" in ice patches in the southern Yukon.

Correlation of Ice Patch Mass Balance and Palaeoclimate in the NWT

In addition to controls on snow drifting (topography and wind direction), the mass balance of NWT ice patches depends on winter accumulation and summer ablation.

Winter accumulation is determined by the amount of precipitation. Consequently, accumulation is limited during exceedingly cold winters, when air moisture content drops. Summer ablation is dependent on air temperature. Thus, like the perennial snow patches studied by Higuchi (1975), NWT ice patches grow during periods when winter has high precipitation and summer is cool. Periods of low or negative growth would be characterized by dry winters, warm summers, or both. Our data reveal that winter accumulation is equal to or less than summer ablation most years, but these are interspersed with limited years of large net accumulation. Thus, ice patch growth is discontinuous and occurs intermittently. This discontinuous model of ice body growth has resulted in only 2.8 m of ice accumulation at KfTe-1 over the last 4420 years and ~1.4 m of ice accumulation at KhTe-2 over 3270 years.

During the Early Holocene (10 000–5000 years BP), NWT climate was warmer than present. Kaufman et al. (2004) suggest that average summer temperatures were 1.6 ± 0.8°C warmer in circumpolar regions. East of the study area in the Mackenzie River Basin, the modern distribution of freshwater invertebrates suggests that mean annual temperature may have been as much as 8.2–11.6°C warmer than at present (Delorme et al., 1977). In the Mackenzie Mountains, the boreal forest reached a maximum density around 5000 years BP and extended approximately 50 km northward beyond the modern tree line (Ritchie, 1984), which also indicates a warming trend. This warm regional climate during the Early Holocene interrupted snow accumulation and ice patch formation at KfTe-1 and KhTe-2. These NWT ice patches are similar to those in the southern Yukon, where there was no net accumulation for the interval 6700–4700 years BP because of relatively high air temperatures, reduced precipitation, or both (Farnell et al., 2004).

The beginning of the Late Holocene (5000 years BP to present) was marked by a climatic shift (Menounos et al., 2009). The tree line began to recede in the Mackenzie River Basin, and the muskeg that is typical of the present landscape started to form (MacDonald, 1987; Vardy et al., 1998). In the O'Grady Lake region of the Mackenzie and Selwyn Mountains, a decline in spruce after 5000 years BP indicates a cooler and dryer climate (MacDonald, 1983). Cooling led to permafrost expansion and increased peat development in the Mackenzie region (Zoltai and Tamocai, 1975). The transition from the warmer Early Holocene to a cooler climate at the beginning of the Late Holocene coincides with the earliest radiocarbon dates recovered from KfTe-1. Around 4500 years BP, cooler summer temperatures allowed the accumulation of snow to persist as the ice patch developed. It is possible that a prior ice patch existed in this location but was lost. The average rate of ice accumulation for the first 500 years of the KfTe-1 ice patch is relatively low, probably because of dry climatic conditions at that time.

Ice patches differ from glaciers in that they do not acquire enough mass to move downslope, yet their main accumulation control (precipitation) is the same. Thus ice patches, like glaciers, expand or contract with changes in the average accumulation rate. It is possible to correlate the activity of glaciers and ice patches. In the Coast Mountains to the west, Holocene glaciers have undergone major periods of advance and retreat (Menounos et al., 2009). A significant peak in the average accumulation rate at KfTe-1 roughly coincides with a period of glacial expansion from 3540–2770 years BP. However, the KfTe-1 accumulation rate declines rapidly around 2900 years BP, a period when glacial advances were still taking place in the St. Elias Mountains of the Yukon and the Canadian Rocky Mountains of British Columbia (Denton and Stuiver, 1966; Luckman et al., 1993). While the oldest radiocarbon dates recovered from KhTe-2 are on the order of 3300 years BP, the average accumulation rate is low at both ice patches between 2900 and 1900 years BP. This pattern is at odds with the climate conditions in the Mackenzie Delta after 3000 years BP, which have been described as relatively stable, cool, and moist (Ritchie, 1984, 1985; Vardy et al., 1998). Possibly this disparity indicates regional variations caused by short-term warming events superimposed on long-term climatic fluctuations. Such events, such as a single hot and sunny summer, can result in high ablation rates, so that a catastrophic melt can erase a long period of accumulation.

Average accumulation rates begin to rise at KfTe-1 around 1900 years BP and at KhTe-2 around 1700 years BP, and these dates may be correlated with a period of glacial advance in the Coast Mountains at 1710 years BP (Menounos et al., 2009). A correlation between rising accumulation rates and glacial advance could increase our understanding of the extent of past climate variations. As in the Yukon ice patches, higher rates of average ice accumulation at KfTe-1 and KhTe-2 over the last 1000 years likely culminated with the Little Ice Age (LIA) (Farnell et al., 2004). In the Mackenzie Delta, air temperatures during the LIA were about 1°C cooler (Bégin et al., 2000). Most glaciers reached their LIA maximum extents between AD 1830 and AD 1880 (Menounos et al., 2009). Clague et al. (2009) found that in western Canada and elsewhere, significant glacier recession did not begin until the early to mid-20th century. Aerial photographs from 1949 show that KfTe-1 and KhTe-2 were substantially larger than their present extent. At KfTe-1, former ice patch extent is revealed by large unvegetated areas immediately upslope and to the north (Fig. 2). Such a rapid decrease in mass is probably due to a ~3°C increase in summer air temperature in the NWT over the past 50 years (Chapman and Walsh, 2003).

Mountain glaciers are sensitive to climatic changes and respond by adjusting their width, length, and thickness (Menounos et al., 2009). The response time for glaciers, however, can range from several years to decades (Jóhannesson et al., 1989; Chinn, 1999). For KfTe-1 and KhTe-2, where changes in ice patch accumulation rate coincide with mountain glacier activity, it appears that ice patches are quicker to react. The effects of a changing climate—or even individual weather events, like a single warm summer—are more likely to produce changes to the ice patches

because of their limited size and thickness. Such annual changes in ice patch accumulation controls are expressed as annual morphological variation. Snow patches in Scotland and Australia exhibit similar sensitivity to climate and weather variation each year (Watson et al., 1994; Green and Pickering, 2009). Because of their rapid response and ease of measurement, ice patches could be used as indicators of short-term climate change and increasing extreme weather events. It should be noted that while glaciers and ice patches will experience similar effects of some climate mechanisms, they will react quite differently to others. It is, nonetheless, important to introduce the potential significance of ice patches for the larger regional climate history.

The perimeter of KfTe-1 decreased significantly from August 2007 to August 2008 (Fig. 12). Ground-penetrating radar profiles from 2007 and 2008 show that the mass lost was mainly snow, but included some thin underlying ice beyond the thicker section of the patch. Whether or not thin sections persist late into the ablation season is variable. The 2009 perimeter of KfTe-1 is comparable to that of 2007. At KhTe-2, however, the perimeter of the ice patch gradually decreased from 2007 to 2009. Norman Wells weather data (Environment Canada, 2010) show that 2008 was a cooler year and the annual melting degree days (MDD) in 2008 are lowest for the three-year span (MDD: 2007 = 2718 ˚C days; 2008 = 2560 ˚C days; 2009 = 2713 ˚C days). Thus, NWT ice patches are not only influenced by climate variation and weather events on a short temporal scale, but also subject to influences at a fine spatial scale (local to individual ice patches).

CONCLUSIONS

Northwest Territories ice patches are similar in their composition, morphology, and controls to persistent ice features found elsewhere. Ground-penetrating radar and ice cores effectively reveal the internal structure and geometry of NWT ice patches. They are composed of a core of offset ice bodies that form through meltwater percolation and localized firn densification and are covered by a blanket of snow. Caribou dung and sediment, concentrated into layers during catastrophic melt of the upper ice, separate the individual ice bodies. The ice accumulates during periods when winter precipitation is high and the summer is cool, allowing annual depositions of drifting snow to persist. Fluctuations in NWT ice patch accumulation rates coincide with shifts in regional climate. While the NWT ice patches have persisted for thousands of years, their mass balance is highly influenced by local phenomena over short time periods.

ACKNOWLEDGEMENTS

Funding for this research was provided by the Canadian International Polar Year Program. The authors thank Erik Blake, Bernd Kulessa, and two anonymous reviewers for their critical comments. Derek Wilson, Farzin Malekani, and Amy Barker are acknowledged for their assistance.

REFERENCES

Aitken, J.D., and Cook, D.G. 1974. Carcajou Canyon map area, District of Mackenzie, Northwest Territories. Geological Survey of Canada.

Anderson, D.L., and Benson, C.S. 1963. The densification and diagensis of snow. Chapter 30. In: Kingery, W.D., ed. Ice and snow. Massachusetts: The MIT Press. 391–411.

Andrews, T.D., MacKay, G., and Andrew, L. 2009. Hunters of the alpine ice: The NWT Ice Patch Study. Yellowknife: Prince of Wales Northern Heritage Centre, Government of Northwest Territories.

Andrews, T.D., MacKay, G., and Andrew, L. 2012. Archaeological investigations of alpine ice patches in the Selwyn Mountains, Northwest Territories, Canada. Arctic 65(Suppl. 1):1–21.

Annan, A.P. 2001. Ground penetrating radar workshop notes. Mississauga, Ontario: Sensors and Software Inc.

———. 2002. GPR—History, trends, and future developments. Subsurface Sensing Technologies and Applications 3(4):253–270.

Bégin, C., Michaud, Y., and Archambault, S. 2000. Tree-ring evidence of recent climate changes in the Mackenzie Basin, Northwest Territories. In: Dyke, L.D., and Brooks, G.R., eds. The physical environment of the Mackenzie Valley, Northwest Territories: A baseline for the assessment of environmental change. Bulletin 547. Ottawa: Geological Survey of Canada, Natural Resources Canada. 65–77.

Berrisford, M.S. 1991. Evidence for enhanced mechanical weathering associated with seasonally late-lying and perennial snow patches, Jotunheimen, Norway. Permafrost and Periglacial Processes 2(4):331–340.

Billings, W.D., and Bliss, L.C. 1959. An alpine snowbank environment and its effects on vegetation, plant development, and productivity. Ecology 40:388–397.

Blusson, S.L. 1971. Geology, Sekwi Mountain, Map 1333A. Ottawa: Geological Survey of Canada.

Chapman, W.L., and Walsh, J.E. 2003. Observed climate change in the Arctic, updated from Chapman and Walsh, 1993. Recent variations of sea ice and air temperatures in high latitudes. Bulletin of the American Meteorological Society 74:33–47.

Chinn, T.J. 1999. New Zealand glacier response to climate change of the past 2 decades. Global and Planetary Change 22:155–168.

Clague, J.J., Menounos, B., Osborn, G., Luckman, B.H., and Koch, J. 2009. Nomenclature and resolution in Holocene glacial chronologies. Quaternary Science Reviews 28:2231–2238.

Cuffey, K.M., and Paterson, W.S.B. 2010. The physics of glaciers, 4th ed. Oxford: Elsevier.

Daniels, D.J. 1996. Surface-penetrating radar. London: Institution of Electric Engineers.

Davis, C. 1998. Meteorological aspects of snow. In: Green, K., ed. Snow: A natural history; an uncertain future. Canberra: Australian Alps Liaison Committee. 3–34.

Delorme, L.D., Zoltai, S.C., and Kalas, L.L. 1977. Freshwater shelled invertebrate indicators of paleoclimate in northwestern Canada during late glacial times. Canadian Journal of Earth Sciences 14:2029–2046.

Denton, G.H., and Stuiver, M. 1966. Neoglacial chronology, northeastern Saint Elias Mountains, Canada. American Journal of Science 264:577–599.

Duk-Rodkin, A., Barendregt, R.W., Tarnocai, C., and Phillips, F.M. 1996. Late Tertiary to late Quaternary record in the Mackenzie Mountains, Northwest Territories, Canada: Stratigraphy, paleosols, paleomagnetism, and chlorine-36. Canadian Journal of Earth Sciences 33:875–895.

Environment Canada. 2010. Norman Wells monthly data report, 2007–2009. http://www.climate.weatheroffice.gc.ca/climateData/monthlydata_e.html?timeframe=3&Prov=XX&StationID=1680&Year=2009&Month=8&Day=22.

Farnell, R., Hare, P.G., Blake, E., Bowyer, V., Schweger, C., Greer, S., and Gotthardt, R. 2004. Multidisciplinary investigations of alpine ice patches in southwest Yukon, Canada: Palaeoenvironmental and palaeobiological investigations. Arctic 57(3):247–259.

Fujita, S., and Mae, S. 1994. Causes and nature of ice-sheet radio-echo internal reflections estimated from the dielectric properties of ice. Annals of Glaciology 20:80–86.

Galley, R.J., Trachtenberg, M., Langlois, A., Barber, D.G., and Shafai, L. 2009. Observations of geophysical and dielectric properties and ground penetrating radar signatures for discrimination of snow, sea ice and freshwater ice thickness. Cold Regions Science and Technology 57(1):29–38.

Galloway, J.M., Adamczewski, J., Schock, D.M., Andrews, T.D., MacKay, G., Bowyer, V.E., Meulendyk, T., Moorman, B.J., and Kutz, S.J. 2012. Diet and habitat of mountain woodland caribou inferred from dung preserved in 5000-year-old alpine ice in the Selwyn Mountains, Northwest Territories, Canada. Arctic 65(Suppl. 1):59–79.

Glen, J.W. 1955. The creep of polycrystalline ice. Proceedings of the Royal Society of London Series A 228:519–538.

Green, K., and Pickering, C.M. 2009. The decline of snowpatches in the Snowy Mountains of Australia: Importance of climate warming, variable snow, and wind. Arctic, Antarctic, and Alpine Research 41(2):212–218.

Hare, P.G., Greer, S., Gotthardt, R., Farnell, R., Bowyer, V., Schweger, C., and Strand, D. 2004. Ethnographic and archaeological investigations of alpine ice patches in southwest Yukon, Canada. Arctic 57(3):260–272.

Hare, P.G., Thomas, C.D., Topper, T.N., and Gotthardt, R.M. 2012. The archaeology of Yukon ice patches: New artifacts, observations, and insights. Arctic 65(Suppl. 1):118–135.

Hejcman, M., Dvorak, I.J., Kocianova, M., Pavlu, V., Nezerkova, P., Vitek, O., Rauch, O., and Jenik, J. 2006. Snow depth and vegetation pattern in a late-melting snowbed analyzed by GPS and GIS in the Giant Mountains, Czech Republic. Arctic, Antarctic, and Alpine Research 38(1):90–98.

Higuchi, K. 1975. On the relation between mass balance of perennial snow patches and climatic variation in Central Japan. Snow and Ice – Symposium 104:141–143.

Higuchi, K., Iozawa, T., Fujii, Y., and Kodama, H. 1980. Inventory of perennial snow patches in Central Japan. Geojournal 4(4):303–311.

Iida, H., Takenaka, S., Ageta, Y., and Fushimi, H. 1990. Internal structure of ice body of Kuranosuke snow patch in the northern Japanese Alps. In: Higuchi, K., ed. Studies on the structure and formation of the oldest fossil ice body in Japan. Summary report of research project by Grant-in Aid for Scientific Research from Monbusho.

Jackson, L.E., Jr., Ward, B., Duk-Rodkin, A., and Hughes, O.L. 1991. The Last Cordilleran ice sheet in southern Yukon Territory. Géographie physique et Quaternaire 45(3):341–354.

Jóhannesson, T., Raymond, C., and Waddington, E. 1989. Time-scale for adjustment of glaciers to changes in mass balance. Journal of Glaciology 35:355–369.

Kaufman, D.S., Ager, T.A., Anderson, N.J., Anderson, P.M., Andrews, J.T., Bartlein, P.J., Brubaker, L.B., et al. 2004. Holocene thermal maximum in the western Arctic (0–180° W). Quaternary Science Reviews 23:529–560.

Kawashima, K. 1997. Formation processes of ice body revealed by the internal structure of perennial snow patches in Japan. Bulletin of Glacier Research 15:1–10.

Kawashima, K., Yamada, T., and Wakahama, G. 1993. Investigations of internal structure and transformational processes from firn to ice in a perennial snow patch. Annals of Glaciology 18:117–122.

Kershaw, G.P. 1983. Long-term ecological consequences in tundra environments of the CANOL crude oil pipeline project, N.W.T., 1942–1945. PhD thesis, University of Alberta, Edmonton, Alberta.

Klassen, R.W. 1987. The Tertiary-Pleistocene stratigraphy of the Laird Plain, southeastern Yukon Territory. Geological Survey of Canada Paper 86-17. 16 p.

Kuzyk, G.W., Russell, D.E., Farnell, R.S., Gotthardt, R.M., Hare, P.G., and Blake, E. 1999. In pursuit of prehistoric caribou on Thandlät, southern Yukon. Arctic 52(2):214–219.

Lee, C.M. 2012. Withering snow and ice in the mid-latitudes: A new archaeological and paleobiological record for the Rocky Mountain Region. Arctic 65(Suppl. 1):165–177.

Letts, B., Fulton, T.L., Stiller, M., Andrews, T.D., MacKay, G., Popko, R., and Shapiro, B. 2012. Ancient DNA reveals genetic continuity in mountain woodland caribou of the Mackenzie and Selwyn Mountains, Northwest Territories, Canada. Arctic 65(Suppl. 1):80–94.

Luckman, B.H., Holdsworth, G., and Osborn, G.D. 1993. Neoglacial glacier fluctuations in the Canadian Rockies. Quaternary Research 39:144–153.

MacDonald, G.M. 1983. Holocene vegetation history of the Upper Natla River area, Northwest Territories, Canada. Arctic and Alpine Research 15(2):169–180.

———. 1987. Postglacial vegetation history of the Mackenzie River Basin. Quaternary Research 28:245–262.

Macheret, Y.Y., Moskalevsky, M.Y., and Vasilenko, E.V. 1993. Velocity of radio waves in glaciers as an indicator of their hydrothermal state, structure and regime. Journal of Glaciology 39(132):373–384.

McGinley, M. 2008. Ogilvie-Mackenzie alpine tundra. In: Cleveland, C.J., ed. Encyclopedia of Earth. Washington, D.C.: Environmental Information Coalition, National Council for Science and the Environment.

Menounos, B., Osborn, G., Clague, J.J., and Luckman, B.H. 2009. Latest Pleistocene and Holocene glacier fluctuations in western Canada. Quaternary Science Reviews 28:2049–2074.

Nakamura, T. 1990. The C^{14} dating with tandetron accelerator system of the plant samples in ice body of Kuranosuke snow patch in the northern Japanese Alps. In: Higuchi, K., ed. Studies on the structure and formation of the oldest fossil ice body in Japan. 31–42.

Ogasahara, K. 1964. Characteristics of the glaciers in the Japanese Alps at the time of the glacial age (in Japanese). The Nature of the Northern Japan Alps, Toyama University. 5–34.

Pälli, A., Kohler, J.C., Isaksson, E., Moore, J.C., Pinglot, J.F., Pohjola, V.A., and Samuelsson, H. 2002. Spatial and temporal variability of snow accumulation using ground-penetrating radar and ice cores on a Svalbard glacier. Journal of Glaciology 48(162):417–424.

Pälli, A., Moore, J.C., and Rolstad, C. 2003. Firn-ice transition-zone features of four polythermal glaciers in Svalbard seen by ground-penetrating radar. Annals of Glaciology 37(1):298–304.

Paren, J.G., and Robin, G.d.Q. 1975. Internal reflections in polar ice sheets. Journal of Glaciology 14(71):251–259.

Plewes, L.A., and Hubbard, B. 2001. A review of the use of radio-echo sounding in glaciology. Progress in Physical Geography 25(2):203–236.

Reimer, P.J., Baillie, M.G.L., Bard, E., Bayliss, A., Beck, J.W., Blackwell, P.G., Bronk Ramsey, C., et al. 2009. IntCal09 and Marine09 radiocarbon age calibration curves, 0–50,000 years cal BP. Radiocarbon 51(4):1111–1150.

Ren, J., Qin, D., Petit, J.R., Jouzel, J., Wang, W., Liu, C., Wang, X., Qian, S., and Wang, X. 1995. Glaciological studies on Nelson Island, South Shetland Islands, Antarctica. Journal of Glaciology 41(138):408–412.

Ritchie, J.C. 1984. A Holocene pollen record of boreal forest history from the Travaillant Lake area, lower Mackenzie River Basin. Canadian Journal of Botany 62:1385–1392.

———. 1985. Late-Quaternary climatic and vegetational change in the lower Mackenzie Basin, Northwest Canada. Ecology 66:612–621.

Sakai, H., Ura, Y., Nakano, T., Iida, H., and Muroi, K. 2006. Study of the internal structure of the Kuranosuke snow patch in central Japan using ground penetrating radar survey. Bulletin of Glaciological Research 23:77–84.

Sharp, R.P. 1951. Meltwater behaviour in firn on upper Seward Glacier, St. Elias Mountains, Canada. Institute for Advanced Studies in the Humanities Publications 32:246–253.

Siegert, M.J., and Hodgkins, R. 2000. A stratigraphic link across 1100 km of the Antarctic ice sheet between the Vostok ice-core site and Titan Dome (near South Pole). Geophysical Research Letters 27(14):2133–2136.

Stuiver, M., Reimer, P.J., and Reimer, R.W. 2005. CALIB radiocarbon calibration, Version 6.0: Marine reservoir correction database. http://calib.qub.ac.uk/calib/.

Szeicz, J.M., MacDonald, G.M., and Duk-Rodkin, A. 1995. Late Quaternary vegetation history of the central Mackenzie Mountains, Northwest Territories, Canada. Palaeogeography, Palaeoclimatology, Palaeoecology 113:351–371.

Vallon, M., Petit, J.-R., and Fabre, B. 1976. Study of an ice core to the bedrock in the accumulation zone of an alpine glacier. Journal of Glaciology 17(75):13–28.

VanderHoek, R., Dixon, E.J., Jarman, N.L., and Tedor, R.M. 2012. Ice patch archaeology in Alaska: 2000–10. Arctic 65(Suppl. 1):153–164.

Vardy, S.R., Warner, B.G., and Aravena, R. 1998. Holocene climate and the development of a subarctic peatland near Inuvik, Northwest Territories, Canada. Climatic Change 40(2):285–313.

Wahl, H.E., Fraser, D.B., Harvey, R.C., and Maxwell, J.B. 1987. Climate of Yukon. Ottawa: Environment Canada, Atmospheric Environment Service, Climatological Studies.

Wakahama, G., and Narita, H. 1975. Metamorphism from snow to firn and ice in a small snow patch on Mt. Daisetsu, Hokkaido, Japan. Snow and Ice – Symposium 104:347–350.

Washburn, A.L. 1979. Geocryology. London: Edward Arnold.

Watson, A., Davison, R.W., and French, D.D. 1994. Summer snow patches and climate in northeast Scotland, U.K. Arctic and Alpine Research 26(2):141–151.

Watts, R.D., and Wright, D.L. 1981. Systems for measuring thickness of temperate and polar ice from the ground or from the air. Journal of Glaciology 27(97):459–469.

Woodward, J., and Burke, M.J. 2007. Applications of ground-penetrating radar to glacial and frozen materials. Journal of Environmental & Engineering Geophysics 12(1):69–85.

Yamamoto, K., and Yoshida, M. 1987. Impulse radar sounding of fossil ice within the Kuranosuke perennial snow patch, central Japan. Annals of Glaciology 9:218–220.

Yoshida, M., Fushimi, H., Ikegami, K., Takenaka, S., Takahara, S., and Fujii, Y. 1983. Distribution and shape of the vertical holes formed in a perennial ice body of the Kuranosuke snow patch, central Japan. Seppyo (Journal of the Japanese Society of Snow and Ice) 45:25–32.

Zoltai, S.C., and Tarnocai, C. 1975. Perennially frozen peatlands in the western Arctic and Subarctic of Canada. Canadian Journal of Earth Sciences 12:28–43.